

Flash-Heating of Circumstellar Clouds by Gamma Ray Bursts

Charles D. Dermer¹ & Markus Böttcher^{2,3}

ABSTRACT

The blast-wave model for gamma-ray bursts (GRBs) has been called into question by observations of spectra from GRBs that are harder than can be produced through optically thin synchrotron emission. If GRBs originate from the collapse of massive stars, then circumstellar clouds near burst sources will be illuminated by intense γ radiation, and the electrons in these clouds will be rapidly scattered to energies as large as several hundred keV. Low-energy photons that subsequently pass through the hot plasma will be scattered to higher energies, thus hardening the intrinsic spectrum. This effect resolves the “line-of-death” objection to the synchrotron shock model. Illuminated clouds near GRBs will form relativistic plasmas containing large numbers of electron-positron pairs that can be detected within ~ 1 -2 days of the explosion before expanding and dissipating. Localized regions of pair annihilation radiation in the Galaxy would reveal past GRB explosions.

Subject headings: gamma rays: bursts – massive stars – nonthermal radiation processes

1. Introduction

The identification of flaring and fading X-ray, optical and radio counterparts to gamma-ray burst (GRB) sources (e.g., Costa et al. 1997; van Paradijs et al. 1997; Djorgovski et al. 1997; Frail et al. 1997), and the large energy releases implied by redshift measurements, find a consistent explanation in an expanding relativistic blast-wave model (Paczynski & Rhoads 1993; Mészáros & Rees 1997). As a result of Beppo-SAX and optical follow-on observations, the redshifts of about one dozen GRBs with durations greater than ~ 1 s have been measured. The distribution of redshifts is broad and centered near $z \sim 1$, corresponding to the cosmological epoch of active star formation (Hogg & Fruchter 1999). GRBs are extremely luminous and energetic at hard X-ray and γ -ray energies. The degree of GRB collimation is unknown, but peak directional γ -ray luminosities and energy releases as large as $\partial L / \partial \Omega \simeq 3 \times 10^{51}$ ergs (s-sr)⁻¹ and $\partial E / \partial \Omega \simeq 3 \times 10^{53}$ ergs sr⁻¹, respectively, have been measured (Kulkarni et al. 1999). Less powerful GRBs and less

¹E. O. Hulburt Center for Space Research, Code 7653, Naval Research Laboratory, Washington, DC 20375-5352

²Department of Space Physics and Astronomy, Rice University, Houston, TX 77005-1892

³Chandra Fellow

luminous episodes during the GRB produce smaller γ -ray powers, but the apparent isotropic γ -ray luminosities from typical GRBs could regularly reach values exceeding $10^{50} L_{50}$ ergs s $^{-1}$ with $L_{50} \sim 1$, with some GRBs reaching $L_{50} > 10^2$. Because the energy radiated in γ rays is less than the total energy released by a GRB, the apparent isotropic energy release of GRB sources could often reach values of $10^{54} E_{54}$ ergs, with $E_{54} \sim 1$.

Cosmological gamma-ray burst and afterglow observations are best explained through the fireball/blast-wave model, where the deposition of large quantities of energy into a small region yields a fireball that expands until it reaches a relativistic speed determined by the amount of baryons mixed into the fireball (see, e.g., Piran 1999 for a review). Nonthermal synchrotron radiation from energetic electrons in the relativistic blast wave is thought to account for the origin of the prompt γ -ray emission and afterglow radiation. This paradigm has been called into question, however, by observations of very hard X-ray emission during the prompt γ -ray luminous phase of a significant number of GRBs (Crider et al. 1997; Preece et al. 1998). Photon fluxes $\phi(\epsilon) \propto \epsilon^{-\alpha_X}$ with $\alpha_X \sim 0$, where $\epsilon = h\nu/m_e c^2$ is the dimensionless photon energy, have been observed in 5-10% of GRBs that are bright enough to permit spectral analysis. This strongly contradicts the optically-thin synchrotron shock model, which predicts that only radiation spectra with $\alpha_X \geq 2/3$ can emerge from the blast wave. In view of the severity of this challenge to the model, these observations have been termed the “line-of-death” to the synchrotron shock model. Possible explanations for this phenomenon involve photoelectric absorption by optically thick cold matter (Liang & Kargatis 1994; Brainerd 1994; Böttcher et al. 1999), synchrotron self-absorption (Crider & Liang 1999, Granot, Piran, & Sari 2000, Lloyd & Petrosian 1999), Compton scattering (Liang 1997; Liang et al. 1999), or the existence of a pair-photosphere (Mészáros & Rees 2000) within the blast wave. Except for the last model cited, these explanations are inconsistent with the standard synchrotron shock model. Here we offer a solution to this problem that is consistent with the standard model and recent observations pointing to a massive star origin of GRBs.

2. Massive Star Origin of GRBs

Considerable evidence linking the sources of GRBs with star-forming regions has recently been obtained (e.g., Lamb 1999). For example, the associated host galaxies have blue colors, consistent with galaxy types that are undergoing active star formation. GRB counterparts are found within the optical radii and central regions of the host galaxies (e.g. Bloom et al. 1999a), rather than far outside the galaxies’ disks, as might be expected in a scenario of merging neutron stars and black holes (Narayan, Paczyński, & Piran 1992). Lack of optical counterparts in some GRBs could be due to extreme reddening from large quantities of gas and dust in the host galaxy. This, together with the appearance of supernova-like emissions in the late time optical decay curves of a few GRBs (e.g., Bloom et al. 1999b) and weak X-ray evidence for Fe K $_{\alpha}$ -line signatures (Piro et al. 1999), supports a massive star hypernova/collapsar (Woosley 1993; Paczyński 1998) origin for the long duration gamma-ray bursters.

The observations thus favor a model for GRBs involving the collapse of the core of a $\gtrsim 30M_\odot$ star to a black hole, with the collapse events producing fireballs and relativistic outflows with large directed energy releases. Earlier treatments of the blast-wave model considered systems where the density of the surrounding medium is either uniform or monotonically decreasing as a result of a circumstellar medium formed by a hot stellar wind (Mészáros, Rees, & Wijers 1998). Until recently (Chevalier & Li 1999; Li & Chevalier 1999), less attention has been paid to the actual environment found in the vicinity of massive stars. For this we consider η Carinae (Davidson & Humphreys 1997), the best-studied massive star that might correspond to a GRB progenitor. It is an evolved star with present-day mass $\geq 90M_\odot$, distance of 2300 ± 200 pc, and lifetime of about 3 million years. It anisotropically ejects mass at a current rate of $\lesssim 0.003M_\odot \text{ yr}^{-1}$ to form its unusual “homunculus nebula.” Several Solar masses of material surround η Carinae. In the immediate vicinity of the central star, dense clouds of slow-moving gas with radii $r \sim 10^{15}$ cm and densities between 10^7 and 10^{10} cm^{-3} were discovered with speckle techniques (Hofman & Weigelt 1988) and confirmed with high-resolution HST observations (Davidson et al. 1995). This material, moving with speeds of $\sim 50 \text{ km s}^{-1}$, is apparently ejected nonuniformly from the equatorial zone, but may remain trapped by the gravitational field of the star. Inferences (Davidson & Humphreys 1997) from [FeII] observations suggest that $\gtrsim 0.02M_\odot$ of gas are contained within $\sim 2 \times 10^{16}$ cm, implying a volume-averaged gas density $\gtrsim 7 \times 10^5 \text{ cm}^{-3}$. Model results (Böttcher 1999) imply that a dense ($n \sim 10^{12} \text{ cm}^{-3}$) torus of gas at mean distance $d \sim 2 \times 10^{15}$ cm and with a 10-fold enhancement of Fe relative to Solar abundance is required to explain the Fe K_α emission weakly detected from GRB 970508 with Beppo-SAX (Piro et al. 1999).

Guided by the optical observations of η Carinae, we assume that the volume-averaged density of gas at $d \lesssim 10^{16}$ cm of a GRB source is $\langle n \rangle = 10^6 n_6 \text{ cm}^{-3}$. Dense clouds of radius $10^{15} r_{15}$ cm and radial Thomson depths $\tau_T = n_c \sigma_T r$ are assumed to be embedded within this region, so that the mean density of particles in a cloud is $n_c = 1.5 \times 10^9 \tau_T / r_{15} \text{ cm}^{-3}$. Thus $\tau_T \sim 1$ clouds located very close to a GRB source are consistent with the observations of dense blobs near η Carinae. The deceleration length scale of a blast wave with initial Lorentz factor $\Gamma_0 = 100\Gamma_2$ in a uniform medium is $x_d = (3E_0/4\pi\Gamma_0^2\langle n \rangle m_p c^2)^{1/3} = 2.5 \times 10^{15} (E_{54}/\Gamma_2^2 n_6)^{1/3}$ cm; hence the blast wave would emit a significant fraction of its energy before reaching distances of $\sim 10^{16}$ cm. The deceleration time, which corresponds to the duration of the prompt γ -ray luminous phase of a GRB in the external shock model (Rees & Mészáros 1992), is $t_d = (1+z)x_d/(c\Gamma_0^2) \cong 8(1+z)(E_{54}/\Gamma_2^8 n_6)^{1/3}$ s. These parameters are not unique, and we expect that GRBs display a wide range of energies, Lorentz factors and surrounding mean densities that could accommodate the diverse range of GRB observations.

3. Blast-Wave/Cloud Interaction

A wave of photons impinging on a cloud located $10^{16} d_{16}$ cm from the explosion center will photoionize and Compton-scatter the ambient electrons to energies characteristic of the

incident γ rays (Madau & Thompson 1999). The γ -ray photon front has a width of ~ 10 -100 lt-s, corresponding to the duration of the GRB, whereas the plasma cloud has a width of $\sim 3 \times 10^4 r_{15}$ lt-s, so that the radiation effects must be treated locally. The radiation force driving the electrons outward is balanced by strong electrostatic forces from the more massive protons and ions that anchor the system until the net impulse is sufficient to drive the entire plasma cloud outward. The Compton back-scattered photons provide targets for successive waves of incident GRB photons through $\gamma\gamma$ pair-production interactions (Thompson & Madau 1999). Higher-energy photons are preferentially attenuated, forming an additional injection source of $\gtrsim 1$ MeV electron-positron pairs. The nonthermal electrons and pairs will Compton scatter successive waves of photons, thereby modifying the incident spectrum. The pairs, no longer bound by electrostatic attraction with the ions, will be driven outward by both radiation forces and restoring electrostatic fields to form a mildly relativistic pair wind passing through the more slowly moving normal plasma. Shortly after the γ -ray photon front has passed, the decelerating blast wave from the GRB will plow into the cloud, shock-heating the relativistic plasma.

Nonthermal synchrotron photons with energy ϵ impinge on the atoms in the cloud with a flux which can be parametrized as

$$\Phi(\epsilon) = (4\pi d^2)^{-1} \frac{L}{m_e c^2 \epsilon_0^2 \zeta_1} \left[\frac{1}{(\epsilon/\epsilon_0)^{2/3} + (\epsilon/\epsilon_0)^{\alpha_\gamma}} \right] \quad (1)$$

(Dermer, Chiang, & Böttcher 1999), where $\epsilon_0 \sim 1$ is the photon energy of the peak of the νF_ν spectrum, $\alpha_\gamma \sim 2$ -3 is the photon spectral index at energies $\epsilon \gg \epsilon_0$, and $\zeta_1 \cong [3/4 + (\alpha_\gamma - 2)^{-1}]$. Hydrogen, the most abundant species in the cloud, will be ionized on a time scale of $5 \times 10^{-5} (1+z) d_{16}^2 \zeta_1 \epsilon_0^{4/3} / L_{50}$ s. Fe features might persist briefly during the early periods of very weak GRBs on a time scale of $4 \times 10^{-3} (1+z) d_{16}^2 \zeta_1 \epsilon_0^{4/3} / L_{50}$ s, and would be identified by a rapidly evolving Fe absorption feature at $9.1/(1+z)$ keV. After the H and Fe are ionized, the coupling between the GRB photons and gas is dominated by Compton scattering interactions. Pair production through photon-particle processes are negligible by comparison with Compton interactions except for photons with $\epsilon \gtrsim 200$. A lower limit to the time scale for an electron to be scattered by a photon is $t_T(s) \approx 15(1+z) d_{16}^2 \zeta_1 \epsilon_0 / \zeta_2 L_{50}$, where $\zeta_2 = [3 + (\alpha_\gamma - 1)^{-1}]$, assuming that all Compton scattering events occur in the Thomson limit. The Klein-Nishina decline in the Compton cross section will increase this estimate by a factor of ~ 1 -3, depending on the incident spectrum. Most of the electrons in the cloud will therefore be scattered to high energies during a very luminous ($L_{50} \gg 1$) GRB, or when the cloud is located at $d_{16} \ll 1$.

The average energy transferred to an electron at rest when Compton-scattered by a photon with energy ϵ is $\Delta\epsilon \cong \epsilon^2 / (1 + 1.5\epsilon)$ (this expression is accurate to better than 18% for $\epsilon < 10^3$). Defining $\eta = \gamma - 1$ as the dimensionless electron kinetic energy, we can easily estimate the production rate $f(\eta)$ of electrons scattered to energy η in the nonrelativistic ($\eta \ll 1$) and extreme relativistic ($\eta \gg 1$) limits, noting that $f(\eta)d\eta \propto \Phi(\epsilon)\sigma_C(\epsilon)d\epsilon$ and letting $\eta \cong \Delta\epsilon$. In the former limit, the Compton cross section $\sigma_C(\epsilon) \rightarrow \sigma_T$ and $\Phi(\epsilon) \propto \epsilon^{-2/3}$, so that $f(\eta) \propto \eta^{-5/6}$ when $\eta \ll \min(1, \epsilon_0^2)$. In the high energy limit, $\sigma_C(\epsilon) \propto \ln(3.3\epsilon)/\epsilon$ and $\Phi(\epsilon) \propto \epsilon^{-\alpha_\gamma}$, so that

$f(\eta) \propto \eta^{-(\alpha_\gamma+1)} \ln(2.2\eta)$ when $\eta \gg \max(1, \epsilon_0^2)$. Thus electrons are Compton-scattered on the time scale derived above to form a hard spectrum that turns over at kinetic energies of $\gtrsim 500 \times \min(1, \epsilon_0^2)$ keV. For a GRB with $\epsilon_0 \sim 1$, most of the kinetic energy is therefore carried by nonthermal electrons with energies of ~ 500 keV. Successive waves of photons that pass through this plasma will continue to Compton-scatter the nonthermal electrons. Only the lowest energy photons, however, will be strongly affected by the radiative transfer because both the Compton scattering cross section and energy change per scattering is largest for the lowest energy photons.

Following the initial wave of photons, successive photon fronts also encounter the back-scattered radiation (Madau & Thompson 1999; Thompson & Madau 1999). The kinematics of the Compton process dictate that the energy ϵ_s of a photon back-scattered through 180° by an electron at rest is $\epsilon_s = \epsilon/(1+2\epsilon)$; thus ϵ_s cannot exceed $1/2$ the electron rest-mass energy. Head-on collisions of the back-scattered photons by primary GRB photons with $\epsilon_1 > 2/\epsilon_s = 2 + 2\sqrt{3}$ can thus produce nonthermal e^+e^- pairs. The cross section for $\gamma\gamma$ pair production peaks near threshold with a value of $\sim \sigma_T/3$. The $\gamma\gamma$ pair-production optical depth $\tau_{\gamma\gamma}(\epsilon_1)$ of a photon that trails the onset of the GRB by Δt seconds can be estimated by noting that the photon traverses a distance $\sim r$ through a backscattered radiation field of spectral density $n_s(\epsilon_s) \approx n_e \sigma_T \cdot \Delta t \cdot \Phi[\epsilon_s/(1-2\epsilon_s)]$ – a more accurate calculation would replace the term $\Delta t \cdot \Phi[\epsilon_s/(1-2\epsilon_s)]$ by an integral over the time-varying flux. Approximating $\tau_{\gamma\gamma}(\epsilon_1) \approx r(\sigma_T/3)\Delta\epsilon_s n_s(2/\epsilon_1)$, where $\Delta\epsilon_s \simeq 2/\epsilon_1$ is the bandwidth that is effective for producing pairs, we obtain

$$\tau_{\gamma\gamma}(\epsilon_1) \approx 0.02 \frac{\tau_T \Delta t [s] L_{50} k(\epsilon_1)}{d_{16}^2 \epsilon_1 \epsilon_0^2 \zeta_1} \left[\frac{1}{(\epsilon'/\epsilon_0)^{2/3} + (\epsilon'/\epsilon_0)^{\alpha_\gamma}} \right], \quad (2)$$

where $\epsilon' = 2/(\epsilon_1 - 4)$. The coefficient results from a more detailed derivation, and the term $k(\epsilon_1) = 1 - 4\epsilon_1^{-1} + \epsilon_1/(\epsilon_1 - 4)$ is a Klein-Nishina correction. Eq. (2) shows that photons with energies above several MeV will be severely attenuated in Thomson thick clouds if $L_{50} \gg 1$ or $d_{16} \ll 1$. Photons with MeV energies are most severely attenuated, and $\tau_{\gamma\gamma}(\epsilon_1) \propto \epsilon_1^{-1/3}$ at energies $\epsilon_1 \gg \max(1, \epsilon_0)$. The $\gamma\gamma$ pair injection process provides another source of nonthermal leptons with $\eta \sim 1$. The pairs will not, however, be electrostatically bound but will be accelerated by the photon pressure and electrostatic field.

Fig. 1 shows Monte Carlo simulations of radiation spectra described by eq. (1) that pass through a hot electron scattering medium. For simplicity, we approximate the hard nonthermal electron spectrum by a thermal distribution with temperatures of 100 and 300 keV. These calculations show that the lowest energy photons of the primary synchrotron spectrum are most strongly scattered, and that the “line-of-death” problem of the synchrotron shock model of GRBs (Preece et al. 1998) can be solved by radiation transfer effects through a hot scattering cloud with $\tau_T \gtrsim 1-2$.

According to this interpretation, GRBs displaying very hard spectra could display one break from the intrinsic synchrotron shock spectrum and a second break from the scattering process. In the examples shown in Fig. 1, these two breaks are so close to each other that they appear as one smooth turnover. Two breaks are observed from GRB 970111 (Crider & Liang 1999), a GRB that

strongly violates the “line of death.” A prediction of this model is that GRBs showing such flat X-ray spectra should also display softer MeV spectra than typical GRBs due to $\gamma\gamma$ attenuation processes in the hot scattering cloud.

4. Observational Signatures of the Flash-Heated Cloud

The Compton-scattered electrons transfer momentum to the $N_p = 4 \times 10^{54} r_{15}^3 n_9$ protons of the cloud through their electrostatic coupling. If the radiation efficiency is ξ_r , then the Compton impulse gives each proton in the cloud $\approx \xi_r [1 - \exp(-\tau_T)] E \pi r^2 / (4\pi d^2 N_p) \approx 40 [1 - \exp(-\tau_T)] (\xi_r / 0.1) E_{54} / (d_{16}^2 r_{15} n_9)$ MeV of directed energy. Pairs, by contrast, will be accelerated to mildly relativistic speeds until Compton drag or streaming instabilities limit further acceleration. In the simplification that the medium interior to the cloud is uniform, and neglecting pair-loading of the swept-up material (Thompson & Madau 1999), the decelerating blast wave follows the dynamical equation $\Gamma(x) = \Gamma_0 (x/x_d)^{-g}$, where $g = 3/2$ and 3 for adiabatic and radiative blast waves, respectively. Using the standard parameters adopted here, the blast wave slows to between $\xi = 0.01 - 0.1$ of its initial Lorentz factor before reaching a cloud at $d = 10^{16}$ cm. Even considering the radiative acceleration of the cloud, the blast wave reaches the cloud at time $t_{bw} = t_d (d/x_d)^{(2g+1)/(2g+1)} \lesssim t_{\text{dyn}}$, where the dynamical time scale of the cloud is $t_{\text{dyn}} = r/c = 3 \times 10^4 r_{15}$ s. Because the cloud is so dense, a large fraction of the residual energy of the blast wave is deposited into the N_p particles of the cloud. Thus each proton in the cloud receives an additional $m_p \beta_p^2 c^2 \approx \xi E \pi r^2 / (4\pi d^2 N_p) \approx 40 (\xi / 0.1) E_{54} / (d_{16}^2 r_{15} n_9)$ MeV of kinetic energy, divided roughly equally into directed outflow and random thermal energy.

If the circumstellar medium at $d_{16} \gg 1$ is much more dilute than the interior region, as suggested by observations of η Carinae, then we can neglect further interactions of the cloud/blast wave system with their surroundings. The observational signatures and fate of the cloud at late times can be outlined by comparing time scales. The cloud expands on a time scale $t_{\text{ex}} = t_{\text{dyn}}/\beta = 1.5 \times 10^5 r_{15} / (\beta/0.2)$ s. The basic time scale governing radiative processes in the cloud is the Thomson time $t_T = (n_e \sigma_T c)^{-1} = 5 \times 10^4 / n_9$ s $= t_{\text{dyn}}/\tau_T$. The electrons thermalize on a time scale $t_T / \ln \Lambda \ll t_{\text{dyn}}$, where the Coulomb logarithm $\ln \Lambda \approx 20$. The protons transfer their energy to the electrons on the time scale $t_{ep} \cong \theta^{3/2} (m_p/m_e) t_T / \ln \Lambda$, where $\theta = kT/m_e c^2$ is an effective dimensionless electron temperature, and we assume collective plasma processes for energy exchange to be negligible.

The flash-heated cloud can evolve in two limiting regimes. When the external soft-photon energy density is small, the system emits by a hard bremsstrahlung spectrum with $\theta \sim 1$ and luminosity $L_{ff} \cong N_e \alpha_f m_e c^2 \theta^{1/2} / t_T \approx 5 \times 10^{41} r_{15}^3 n_9^2 \theta^{1/2}$ ergs s $^{-1}$. In the more likely case when abundant soft photons are present, for example, from the Compton echo (Madau, Blandford, & Rees 1999), then Compton cooling will balance ion heating to produce a luminous Comptonized soft-photon spectrum with effective temperature $\theta \sim 0.1$ and luminosity $L_C \cong \xi E \pi r^2 / (4\pi d^2 t_{ep}) \approx 2 \times 10^{45} (\xi / 0.1) E_{54} r_{15}^2 n_9 d_{16}^{-2} (\theta / 0.1)^{-3/2}$ ergs s $^{-1}$. In either case, the

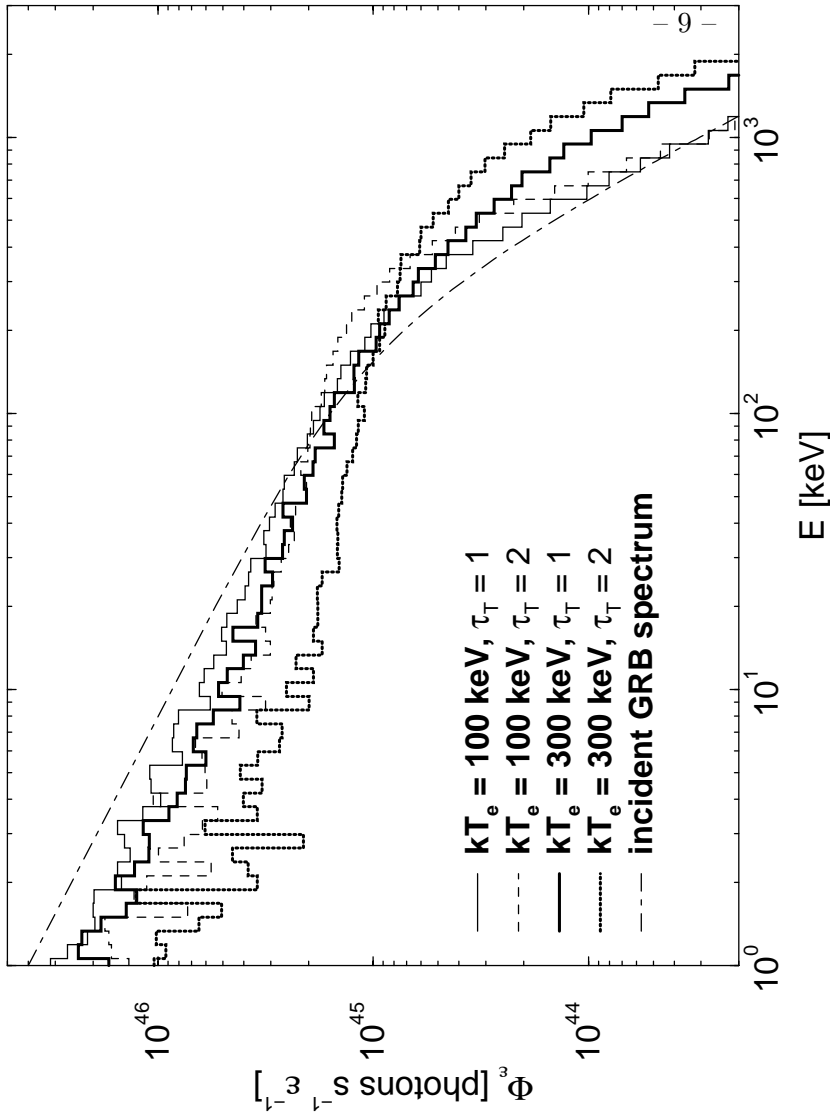
spectra persist until the plasma expands and adiabatically cools, that is, for a period $\sim t_{ex} \sim \text{day}$. The hot bremsstrahlung plasma will be too dim to be detectable with current instrumentation, but a 50-100 keV Comptonized plasma at redshift $z \sim 1$ and luminosity distance of $10^{28} D_{28} \text{ cm}$ would have a flux of $\sim 1.6 \times 10^{-12} (\xi/0.1) E_{54} r_{15}^2 n_9 d_{16}^{-2} (\theta/0.1)^{-3/2} D_{28}^{-2} \text{ ergs cm}^{-2} \text{ s}^{-1}$. The hot plasma formed by a nearby GRB at $z \sim 0.1$ would be easily detectable with the INTEGRAL and Swift missions at hard X-ray and soft γ -ray energies. In either case, e^+e^- pairs would be formed with moderate efficiency, and the cooling, expanding plasma would produce a broad pair annihilation feature (Guilbert & Stepney 1985). The residual pairs formed in the relativistic plasma and the pair wind would diffuse into the dilute interstellar medium with density n_{ISM} to annihilate on a time scale $(n_{\text{ISM}} \sigma_{\text{TC}})^{-1} \sim 2 \times 10^6 / n_{\text{ISM}} \text{ yr}$. If the energy intercepted by a single cloud is converted to pairs with a conservative 1% pair yield, past GRBs in the Milky Way would be revealed by localized regions of annihilation radiation with flux $\sim 2 \times 10^{-5} E_{54} n_{\text{ISM}} (d/10\text{kpc})^{-2} 0.511 \text{ MeV ph cm}^{-2} \text{ s}^{-1}$. The high-latitude annihilation feature discovered with OSSE on the Compton Gamma Ray Observatory (Purcell et al. 1997), or other localized hot spots of annihilation radiation that will be mapped in detail with INTEGRAL, could reveal sites of past GRB explosions.

CD thanks B. Paczyński for stressing the importance of massive star observations in developing blast-wave models of GRBs. The work of CD is supported by the Office of Naval Research and NASA Astrophysical Theory Program (DPR S-13756G). The work of MB is supported by NASA through Chandra Postdoctoral Fellowship grant PF 9-10007, awarded by the Chandra X-ray Center, which is operated by the Smithsonian Astrophysical Observatory for NASA under contract NAS 8-39073.

REFERENCES

- Bloom, J. S. et al. 1999a, *ApJ*, 518, L1
 Bloom, J. S. et al. 1999b, *Nature* 401, 453
 Böttcher, M., Dermer, C. D., Crider, A. W. & Liang, E. P. 1999, *A&A* 343, 111
 Böttcher, M. 1999, *ApJ*, submitted (astro-ph/9912030)
 Brainerd, J. J. 1994, *ApJ*, 428, 21
 Chevalier, R. A., & Li, Z.-Y., 1999, *ApJ*, 520, L29
 Crider, A. et al. 1997, *ApJ* 479, L39
 Crider, A. W., & Liang, E. P. 1999, *A&AS*, 138, 405
 Costa, E. et al. 1997, *Nature*, 387, 783
 Davidson, K., & Humphreys, R. M. 1997, *ARAA*, 35, 1
 Davidson, K. et al. 1995, *AJ*, 109, 1784

- Dermer, C. D., Chiang, J., & Böttcher, M. 1999, *ApJ* 513, 656
- Djorgovski, S. G. et al. 1997, *Nature*, 387, 876
- Frail, D. A., Kulkarni, S. R., Nicastro, L., Feroci, M. & Taylor, G. B. 1997, *Nature* 389, 261
- Granot, J., Piran, T., & Sari, R., 2000, *ApJ*, submitted (astro-ph/0001160)
- Guilbert, P. W., & Stepney, S., 1985, *MNRAS*, 212, 523
- Hofmann, K. H., & Weigelt, G. 1988, *A&A*, 203, L21
- Hogg, D. W., & Fruchter, A. S. 1999, *ApJ* 520, 54
- Kulkarni, S. R. et al. 1999, *Nature* 398, 389
- Lamb, D. Q. 1999, *A&AS*, 138, 607
- Li, Z.-Y., & Chevalier, R. A., 1999, *ApJ*, 526, 716
- Liang, E. P., 1997, *ApJ*, 491, L15
- Liang, E. P., Crider, A. W., Böttcher, M., & Smith, I. 1999, *ApJ* 519, L21
- Liang, E. P., & Kargatis, V. E., 1994, *ApJ*, 432, L111
- Lloyd, N. M., & Petrosian, V., 1999, in proc. of 5th Huntsville Symposium on Gamma-Ray Bursts, AIP proc. in press (astro-ph/9912205)
- Madau, P. & Thompson, C. 1999, *ApJ*, in press (astro-ph/9909060)
- Madau, P., Blandford, R. D., & Rees, M. J. 1999, *ApJ*, submitted (astro-ph/9912276)
- Mészáros, P. & Rees, M. J. 2000, *ApJL*, in press
- Mészáros, P., Rees, M. J. & Wijers, R. A. M. J. 1998, *ApJ* 499, 301
- Mészáros, P., & Rees, M. J. 1997, *ApJ*, 476, 232
- Narayan, R., Paczyński, B., & Piran, T. 1992, *ApJ* 395, L83
- Paczynski, B. 1998, *ApJ*, 494, L4
- Paczynski, B., & Rhoads, J. 1993, *ApJ*, 418, L5
- Piran, T. 1999, *Phys Rpts*, 314, 575
- Piro, L. et al. 1999, *ApJ*, 514, L73
- Preece, R. D. et al. 1998, *ApJ*, 506, L23
- Purcell, W. R., et al. 1997, *ApJ* 491, 725
- Rees, M. J., & Mészáros, P. 1992, *MNRAS*, 258, 41P
- Thompson, C., & Madau, P. 1999, *ApJ*, submitted (astro-ph/9909111)
- van Paradijs, J. et al. 1997, *Nature*, 386, 686
- Woosley, S. E. 1993, *ApJ*, 405, 273



r]

Fig. 1.— Radiation transfer effects on GRB emission that passes through electrons energized by an earlier portion of the photon front. The intrinsic spectrum eq.(1), with $\alpha_X = 2/3$, $\alpha_\gamma = 2.5$ and $\epsilon_0 = 0.5$, is shown by the thick dashed curve. The nonthermal electrons are approximated by a thermal distribution with temperatures of 100 keV (thin curves) and 300 keV (thick curves), and Thomson depths $\tau_T = 1$ (solid curves) and $\tau_T = 2$ (dotted curves). Spectral indices α_X calculated at 50 keV are 0.5 ($T = 100$ keV, $\tau_T = 1$), 0.44 ($T = 300$ keV, $\tau_T = 1$), 0.14 ($T = 100$ keV, $\tau_T = 2$), and 0.05 ($T = 300$ keV, $\tau_T = 2$).

